

Oxyhalogen-sulfur chemistry — Kinetics and mechanism of the oxidation of cysteamine by acidic iodate and iodine

Alice Chanakira, Edward Chikwana, David H. Peyton, and Reuben H. Simoyi

Abstract: The oxidation of cysteamine by iodate and aqueous iodine has been studied in neutral to mildly acidic conditions. The reaction is relatively slow and is heavily dependent on acid concentration. The reaction dynamics are complex and display clock behavior, transient iodine production, and even oligooscillatory production of iodine, depending upon initial conditions. The oxidation product was the cysteamine dimer (cystamine), with no further oxidation observed past this product. The stoichiometry of the reaction was deduced to be $\text{IO}_3^- + 6\text{H}_2\text{NCH}_2\text{CH}_2\text{SH} \rightarrow \text{I}^- + 3\text{H}_2\text{NCH}_2\text{CH}_2\text{S-SCH}_2\text{CH}_2\text{NH}_2 + 3\text{H}_2\text{O}$ in excess cysteamine conditions, whereas in excess iodate the stoichiometry of the reaction is $2\text{IO}_3^- + 10\text{H}_2\text{NCH}_2\text{CH}_2\text{SH} \rightarrow \text{I}_2 + 5\text{H}_2\text{NCH}_2\text{CH}_2\text{S-SCH}_2\text{CH}_2\text{NH}_2 + 6\text{H}_2\text{O}$. The stoichiometry of the oxidation of cysteamine by aqueous iodine was deduced to be $\text{I}_2 + 2\text{H}_2\text{NCH}_2\text{CH}_2\text{SH} \rightarrow 2\text{I}^- + \text{H}_2\text{NCH}_2\text{CH}_2\text{S-SCH}_2\text{CH}_2\text{NH}_2 + 2\text{H}^+$. The bimolecular rate constant for the oxidation of cysteamine by iodine was experimentally evaluated as $2.7 \text{ (mol L}^{-1}\text{)}^{-1} \text{ s}^{-1}$. The whole reaction scheme was satisfactorily modeled by a network of 14 elementary reactions.

Key words: cysteamine, cystamine, Dushman reaction, oligooscillations.

Résumé : L'oxydation de la cystéamine par l'iodate et l'iode aqueux a été étudiée dans des conditions allant de neutre à faiblement acides. La réaction est relativement lente et dépend fortement sur la concentration en acide. La dynamique de la réaction est complexe et présente un comportement d'horloge avec production transitoire d'iode allant jusqu'à une production oligooscillatoire d'iode suivant les conditions initiales. Le produit de l'oxydation est le dimère de la cystéamine, la cystamine, sans oxydation apparente ultérieure de ce produit. On a déduit que, dans les conditions où la cystéamine est en excès la stoechiométrie de la réaction est $\text{IO}_3^- + 6\text{H}_2\text{NCH}_2\text{CH}_2\text{SH} \rightarrow \text{I}^- + 3\text{H}_2\text{NCH}_2\text{CH}_2\text{S-SCH}_2\text{CH}_2\text{NH}_2 + 3\text{H}_2\text{O}$ alors que lorsque l'iodate est en excès, la stoechiométrie de la réaction est de la forme $2\text{IO}_3^- + 10\text{H}_2\text{NCH}_2\text{CH}_2\text{SH} \rightarrow \text{I}_2 + 5\text{H}_2\text{NCH}_2\text{CH}_2\text{S-SCH}_2\text{CH}_2\text{NH}_2 + 6\text{H}_2\text{O}$. On a établi que la stoechiométrie de la réaction d'oxydation de la cystéamine par l'iode aqueux est de la forme $\text{I}_2 + 2\text{H}_2\text{NCH}_2\text{CH}_2\text{SH} \rightarrow 2\text{I}^- + \text{H}_2\text{NCH}_2\text{CH}_2\text{S-SCH}_2\text{CH}_2\text{NH}_2 + 2\text{H}^+$. La valeur établie expérimentalement pour la constante de vitesse bimoléculaire d'oxydation de la cystéamine par l'iode est de $2,7 \text{ (mol L}^{-1}\text{)}^{-1} \text{ s}^{-1}$. On peut faire une modélisation complète du schéma réactionnel sur la base de quatorze réactions élémentaires.

Mots clés : cystéamine, cystamine, réaction de Dushman, oligooscillations.

[Traduit par la Rédaction]

Introduction

Organosulfur compounds dominate much of synthetic, analytical, and medicinal chemistry. Oxidations of organic sulfur compounds appear to be involved in many cellular functions, including regulation of protein synthesis and protection of the cell from oxidative damage (1). Owing to the nucleophilic nature of the thiol group, a better understanding of the biological activities of these compounds can be derived from their oxidation mechanisms. Studies of the oxida-

tion mechanisms of organosulfur compounds have been hampered by the propensity of sulfur chemistry to produce complex and exotic dynamics (2), which are fueled by free-radical mechanisms (3), autoxidations, and production of varied products and intermediates (4, 5). With the sulfur center having an oxidation state range of -2 to $+6$, it is easy for these intermediates to assert themselves.

Cysteamine is a very important biological molecule. Medically known as Cystagon, it can be used as oral therapy for prevention of hypothyroidism and enhances growth in patients with nephropathic cystinosis (6, 7). This is a lysosomal storage disorder that was long considered primarily a renal disease but is now recognized as a systemic disorder that eventually affects many organ systems in children (8). This disorder is characterized by cystine accumulation within cellular lysosomes, and cysteamine converts this disulfide into cysteine and a mixed disulfide, cysteamine-cysteine, which can easily be eliminated from the cystinotic lysosomes, thus effecting depletion of cellular cystine (9).

Received 4 April 2005. Published on the NRC Research Press Web site at <http://canjchem.nrc.ca> on 25 February 2006.

A. Chanakira,¹ E. Chikwana, D.H. Peyton, and R.H. Simoyi.² Department of Chemistry, Portland State University, Portland, OR 97207-0751, USA.

¹Present address: College of St. Catherine, St. Paul, MN 55105, USA.

²Corresponding author (e-mail: rsimoyi@pdx.edu).

Cysteamine and its disulfide, cystamine, can also be used in topical eye drops to dissolve corneal cystine crystals (10).

Cysteamine is an excellent scavenger of $\cdot\text{OH}$ and HOCl ; it also reacts with H_2O_2 and other oxygen-based toxic metabolites (11). In addition to protection against radical damage in DNA, cysteamine can also act as a repair agent for DNA through the formation of the protective RSSR^- , which reacts with the DNA^+ radical ion to regenerate DNA and form cystamine (12). It has been shown that cysteamine and its metabolite hypotaurine are far more likely to act as antioxidants in vivo than is taurine, provided that they are present in sufficient concentration at sites of oxidant generation (13). Cysteamine is oxidized to the sulfinic derivative (hypotaurine) only in the presence of cofactorlike compounds such as sulfide, methylene blue, and hydroxylamine (14). Most metabolic pathways give hypotaurine as a precursor to taurine (15, 16).

In some of our recent work, we examined the reactivity of the cysteamine metabolites: hypotaurine (cysteamine sulfinic acid) and taurine (cysteamine sulfonic acid) (17). Oxidation of hypotaurine by chlorite and chlorine dioxide occurred simultaneously at the sulfur center (giving taurine) and at the nitrogen center (to give the chloramines) (18). On the other hand, taurine is relatively inert to oxidation by chlorine dioxide, a reactive radical species, and acidified bromate (19). When subjected to the strong oxidizing agent HOCl , the C—S bond is not cleaved, and reaction occurs exclusively at the nitrogen center, giving chlorotaurine (17).

The key to understanding the physiological role of cysteamine is through its oxidation pathway: its reactive intermediates and oxidation products. In this manuscript we report on the oxidation of cysteamine by the mild oxidizing agents acidic iodate and aqueous iodine. In a nonenzymatic pathway, could the oxidation of cysteamine yield hypotaurine or go all the way to taurine? Specifically, we are aware that the action of most goitrogenic mechanisms involves the consumption of the iodine atom, which is needed for thyroid activity (20). What then, is the rate and mechanism by which cysteamine reacts with molecular iodine?

Experimental

Materials

Cysteamine hydrochloride (CA, 2-aminoethanethiol hydrochloride) (98%), iodine, potassium iodide (Aldrich), sodium perchlorate (98%) (Acros), cystamine dihydrochloride (MP Biomedical), potassium iodate, perchloric acid (72%), soluble starch, sodium thiosulfate, and hydrochloric acid (Fisher) were used without further purification. The concentration of iodine was determined by standardization against thiosulfate with starch as indicator. This standardization allowed us to evaluate the absorptivity coefficient of iodine at its isosbestic point of 460 nm with triiodide as 770 $(\text{mol L}^{-1})^{-1} \text{cm}^{-1}$. This standardization was carried out before each series of kinetic experiments were performed because of the volatile nature of iodine. CA solutions were prepared just before use and not kept for more than 24 h. All solutions were prepared using distilled-deionized water from a Barnstead Sybron Corporation water purification unit. Inductively coupled plasma mass spectrometry (ICPMS) was used to show that our aqueous reaction media

did not contain enough metal ions to affect the overall reaction kinetics and mechanism (21). The highest metal ion concentration was cadmium at 1.5 ppb, followed by lead at 0.43 ppb.

Methods

All experiments were carried out at 25.0 ± 0.5 °C and at a constant ionic strength of 1.0 mol L^{-1} (NaClO_4). CA, sodium perchlorate, and perchloric acid solutions were mixed in one reactant vessel and iodate (or iodine) solutions in another. All kinetics measurements were performed on a Hi-Tech Scientific SF61–DX2 double mixing stopped-flow spectrophotometer. Spectrophotometric determinations were performed on a PerkinElmer Lambda 25 UV–vis spectrophotometer.

Stoichiometric determinations

The stoichiometry for the $\text{CA}-\text{IO}_3^-$ was determined both in excess iodate and in excess CA. In excess iodate the total oxidizing power was determined by titration. Excess acidified iodide was added to the reaction solution, and the released iodine was titrated against standard thiosulfate. Spectrophotometry was also used to determine the amount of iodine formed in excess iodate by its absorbance at 460 nm. In the I_2 –CA reaction the stoichiometry was determined by titrating standardized iodine solution from a burette into a solution of CA of known strength. The end point, which was enhanced by starch indicator, was detected as the point where the blue-black color lingered.

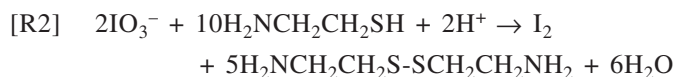
Results

Stoichiometry

The stoichiometry of the reaction was strictly 1:6, with 6 mol of cysteamine reacting with 1 mol iodate. This suggested a one-electron oxidation of the sulfur center, and the only product possible after one-electron oxidation of an organosulfur center was the disulfide ($\text{H}_2\text{NCH}_2\text{CH}_2\text{S}-\text{SCH}_2\text{CH}_2\text{NH}_2$, RSSR). Both spectrophotometric and titrimetric techniques were used to deduce the following stoichiometry:

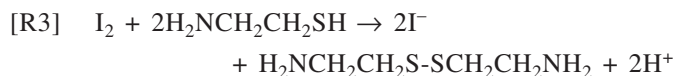


Stoichiometry [R1] was obtained only at the stoichiometric ratio of 1:6. In lower concentrations of iodate, the reaction mixture produced a mixture of both cysteamine and cystamine. These products were confirmed by the NMR spectrum of the mixture. In stoichiometric excess of iodate, the reaction products included iodine, which was then spectrophotometrically examined to deduce the overall stoichiometry of [R2]:



If the iodate-to-substrate ratio was greater than 1:5, then the amount of iodine produced was determined by the amount of cysteamine as the limiting reagent. There was an increase in the amount of iodine produced as the ratio was

increased from 1:6. At 1:5, however, the increase saturated, and no further increase in the production of iodine was observed. The direct reaction of aqueous iodine and cysteamine was determined by a rapid and careful titration aided by starch indicator. Although the end point of the titration shifted upon prolonged standing, the correct stoichiometry was attained at the first end point of 1:2, as shown below.



The complications observed after allowing the titrated solution to incubate arose from two equilibria: the sulfide–disulfide equilibrium (22), which sought to reestablish itself after the depletion of the iodine because of titration with thiosulfate, and the iodine–thiol equilibrium (23, 24), which is well-known and has been extensively discussed in this manuscript under “charge-transfer” complex formation (see below). Stoichiometry [R3] could also be obtained spectrophotometrically in an excess of iodine and under high acid conditions, where both of these complicating equilibria were suppressed.

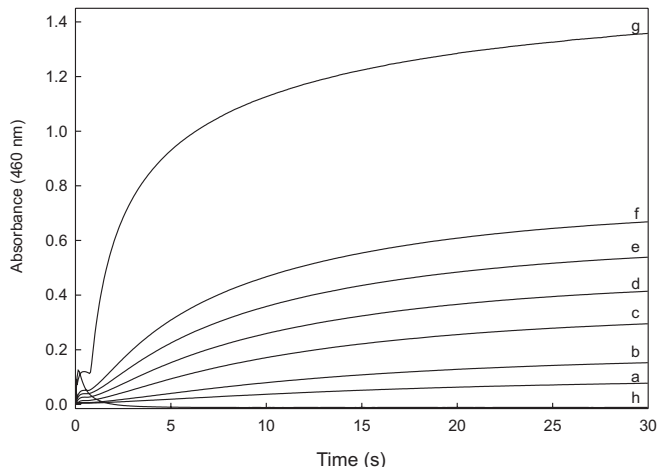
Confirmation of products

Reactions run in excess iodate did not afford sulfate as a product, as shown by the lack of precipitation of barium sulfate with barium chloride. Before barium chloride was added, excess iodate was removed by the use of excess acidified iodide, followed by evaporation of the iodine formed to avoid precipitation of barium iodate. Standard proton NMR spectra were also used to confirm the formation of the disulfide. Reagent grade cysteamine gave the expected spectrum of two triplets owing to the methylene proton sets on the carbon skeleton. This reagent-grade quality cysteamine also showed some cystamine impurity. Addition of DCl destroyed the resolution of the cysteamine triplets and also shifted them downfield because of the protonation of the amino center. The NMR spectrum of the product confirmed that the product was the dimeric cystamine. These product identities were confirmed by an HPLC technique, which utilized an isocratic 98%:2% water–methanol medium. The aqueous medium was 0.05 mol L⁻¹ phosphate at pH 4.0. Both cysteamine and cystamine were modified by addition of acid, and so a control spectrum was initially obtained with cystamine mixed with acid before product UV spectral analyses were performed.

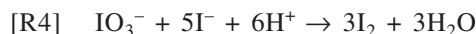
Reaction dynamics

The reaction dynamics were complex, with oligo-oscillatory production of iodine (25), transient formation of iodine, and clock reaction behavior (26). Figure 1 shows all three types of complex dynamics. This is much more evident if the region between $t = 0$ and 5 s is expanded and magnified. Trace h, for example, is at the 1:6 stoichiometric ratio of rxn. [R1] and should produce no aqueous iodine at the end of the reaction. Trace h shows, however, an initial rapid formation of iodine, followed by an equally rapid consumption, all within 3 s. The rest of the traces, a–g, have stoichiometric excess of iodate according to [R1], while only traces a and b have the stoichiometric ratio that satisfies stoichiometry [R2]. Traces a–e display clock reaction characteris-

Fig. 1. CA variation in excess oxidant shows higher rates of iodine production, as well as higher final concentrations of iodine, at the end of the reaction as the CA concentration is increased. Trace h shows that at the stoichiometric ratio there is just a transient formation of iodine. $[\text{IO}_3^-]_0 = 0.005 \text{ mol L}^{-1}$, $[\text{H}^+]_0 = 0.02 \text{ mol L}^{-1}$, $[\text{CA}]_0 =$ (a) 0.0005, (b) 0.001, (c) 0.002, (d) 0.003, (e) 0.004, (f) 0.005, (g) 0.015, (h) 0.03 mol L⁻¹.

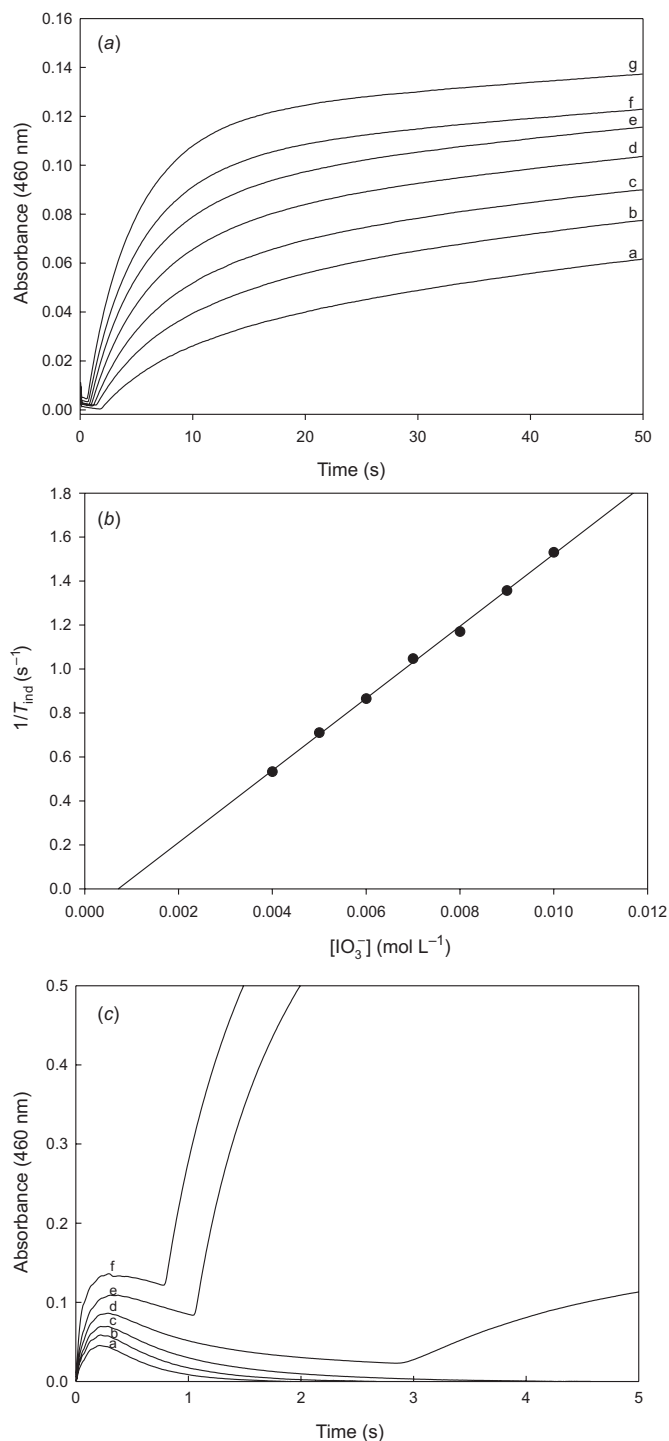


tics: an initial quiescent period followed by formation of iodine. Trace g, on the other hand, shows two peaks in iodine concentrations (oligooscillations), with one peak after approximately 1 s and the other peak (which represented the maximum concentrations obtained) at 60 s (truncated from Fig. 1). The only difference in the traces shown in Fig. 1 is the oxidant-to-reductant ratio, $R = [\text{IO}_3^-]_0/[\text{CA}]_0$. The increase in final iodine concentrations formed in going from trace a to g is justified from the premise that stoichiometry [R2] is a stepwise combination of rxn. [R1] and the Dushman reaction, [R4] ($5[\text{R1}] + [\text{R4}]$) (27).



The collapse of observed iodine concentration in increasing $[\text{CA}]_0$ to trace h arises from the decrease in R (which is $[\text{IO}_3^-]_0/[\text{CA}]_0$) to below that expected for stoichiometry [R2]. Figure 2a shows a series of experimental traces obtained by varying initial iodate concentrations while keeping all other species concentrations constant. Traces c–g satisfy stoichiometry [R2], and thus, at $t = \infty$ all these traces give the same iodine absorbance. Expansion of the first 4 s of the reaction shows a distinct induction period, which could be related to the initial concentration of iodate. We define an induction period as the time taken before a rapid and monotonic formation of iodine commences. A linear relationship (see Fig. 2b) exists between the inverse of this induction period and initial iodate concentrations. The intercept on the iodate axis, the concentration of iodate for an induction period of $t = \infty$ ($1/t = 0$), confirmed stoichiometry [R1]. The intercept is approximately 0.0005 mol L⁻¹ iodate for an initial concentration of 0.003 mol L⁻¹ CA (a 1:6 ratio). An induction time of infinity indicates that no iodine is formed. Any higher iodate concentration over 0.0005 mol L⁻¹ will yield iodine as a final product and stoichiometry will shift from [R1] towards [R2]. In Fig. 2c, increasing the initial acid concentration relative to Fig. 2a and amplifying the first 5 s

Fig. 2. (a) Effect of $[\text{IO}_3^-]$ variation at constant $[\text{H}^+]$ and $[\text{CA}]$ showing a finite and measurable induction period before formation of iodine. The initial rate of reaction increased as $[\text{IO}_3^-]_0$ increased; $[\text{CA}]_0 = 0.003 \text{ mol L}^{-1}$, $[\text{H}^+]_0 = 0.001 \text{ mol L}^{-1}$, $[\text{IO}_3^-]_0 =$ (a) 0.004, (b) 0.005, (c) 0.006, (d) 0.007, (e) 0.008, (f) 0.009, (g) 0.01 mol L^{-1} ; (b) Linear plot of reciprocal induction time vs. $[\text{IO}_3^-]_0$ for data shown in Fig. 2a; (c) Effect of progressively increasing $[\text{IO}_3^-]$ at constant acid and $[\text{CA}]$ close to stoichiometry show oligooscillations. Traces below stoichiometry and at stoichiometry a–c show just the transient formation of iodine. $[\text{CA}]_0 = 0.015 \text{ mol L}^{-1}$, $[\text{H}^+] = 0.02 \text{ mol L}^{-1}$, $[\text{IO}_3^-]_0 =$ (a) 0.0015, (b) 0.002, (c) 0.0025, (d) 0.003, (e) 0.004, (f) 0.005 mol L^{-1} .

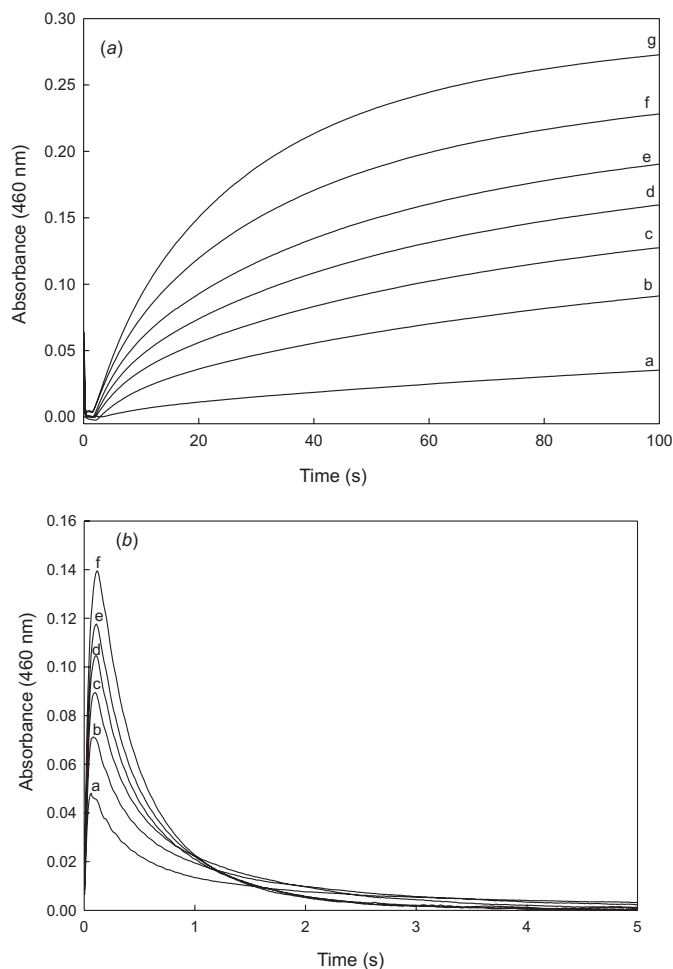


shows, instead of an induction period, a transient peak in iodine concentrations, followed by a final and rapid formation of iodine. In all cases shown in Fig. 2c, the reactions that form iodine initially dominate those that consume iodine (even in stoichiometric excess of CA), and hence the observed initial iodine peak. Iodine formation is also almost instantaneous. The onset of prolonged and monotonic iodine formation is determined by the initial iodate concentrations. For traces e and f, for example, the high ratio ensures rapid consumption of the substrate, leaving only the Dushman reaction, [R4], to form iodine without any other reactions in the reaction medium that consume iodine.

Lower acid concentrations did not produce such oligooscillatory behavior: only a period of no iodine formation is observed, followed by monotonic iodine formation. The strong catalytic effect of acid on the Dushman reaction is responsible for the oligooscillations. The effect of acid on the reaction appears much more complex than that of iodate (see Figs. 3a and 3b). There are several reactions that are viable in this reaction mixture, and it would appear all of them are affected by acid; hence, a clean assessment of the effect of acid is not easily obtained. However, what is obvious from Fig. 3a is that acid concentrations catalyze the formation of iodine after the induction period. In all traces shown in Fig. 3a, the final iodine concentrations were the same ($6 \times 10^{-4} \text{ mol L}^{-1}$, absorbance ~ 0.46). While trace g went to completion in less than 250 s, it took more than 2000 s for trace a to go to completion. A very interesting set of data are shown in Fig. 3b. In this set of data the reaction conditions are set to the stoichiometric ratio of [R1], and at $t = \infty$ no iodine is (nor should be) observed. Acid variations at these conditions show that acid catalyzes the formation of iodine and retards the consumption of iodine. Hence, high acid concentrations will show a wider “excursion” away from the equilibrium conditions before settling down to stoichiometry [R1].

Figure 4 shows the expected catalytic effect of iodide ions. In this case, very low iodide ion concentrations can drastically reduce the induction period (upon expanding the first 2 s of the reaction). They also increase the rate and amount of iodine obtained. This is expected in conditions where the oxidant to reductant ratio (R) is greater than 0.2, where the iodide ions initially added to the reaction mixture combine with those formed in stoichiometry [R1] to fuel the Dushman reaction, [R4]. This is also evident from Fig. 4, which shows a long enough time evolution of the reaction. Other experimental data (not shown) demonstrated a saturation of the reduction of the induction period when the added iodide ions equaled or exceeded the concentrations of the substrate. Iodide acts solely as a catalyst: in stoichiometric excess of the substrate (stoichiometry [R1]), it is used and released intact at the end of the reaction. Iodide ultimately does not participate in the overall stoichiometry except in high excess of iodate conditions, where it is ultimately converted to molecular iodine. Strictly speaking, the Dushman reaction (27) is an extraneous reaction that only asserts itself after stoichiometry [R1] of our fiduciary reaction has been satiated. No simple relationship could be deduced between induction period and (or) rate of formation of iodine with iodide (see Fig. 2b for the iodate dependency). This is due to the fact that the effect of iodide on the whole reaction is

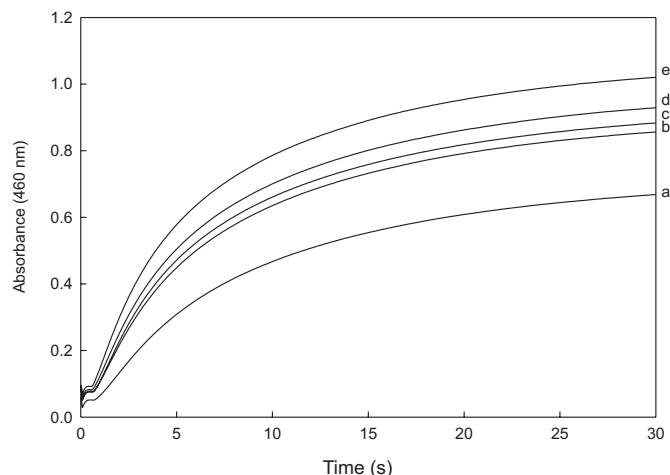
Fig. 3. (a) Effect of varying acid concentration on the oxidation of CA by iodate. There is an increase in rate of iodine formation as acid concentration is increased. $[CA]_0 = 0.003 \text{ mol L}^{-1}$, $[IO_3^-]_0 = 0.003 \text{ mol L}^{-1}$, $[H^+]_0 =$ (a) 0.001, (b) 0.0015, (c) 0.002, (d) 0.0025, (e) 0.003, (f) 0.00375, (g) 0.005 mol L^{-1} ; (b) Effect of acid variation at stoichiometric point (trace h from Fig. 1). The effect of acid can be seen in the form of a higher maximum iodine concentration. $[CA]_0 = 0.03 \text{ mol L}^{-1}$, $[IO_3^-]_0 = 0.005 \text{ mol L}^{-1}$, $[H^+]_0 =$ (a) 0.005, (b) 0.0075, (c) 0.01, (d) 0.0125, (e) 0.015, (f) 0.02 mol L^{-1} .



complex and most likely involves a multiterm rate law. Alternatively (as proved later) iodide ions most likely affect both the formation and consumption of iodine reactions.

The simple and direct oxidation of CA by aqueous iodine was also studied spectrophotometrically at 460 nm. Figure 5a shows that this reaction is relatively slow and is mildly inhibited by acid. Under low acid concentrations, Fig. 5b shows that there is an inverse relationship between the acid concentrations and rate of consumption of iodine. The positive intercept is important: it suggests two pathways, one inhibited by acid and one that is not. The gentle slope of the plot suggests very mild inhibition by acid. This linearity is lost at high acid concentrations (Fig. 5c). The effect of iodide was much more complex (Fig. 6). After mixing iodine and CA, a rapid equilibrium sets up, which forms some adduct that also absorbs at 460 nm. We could not locate a wavelength where this adduct did not adversely affect

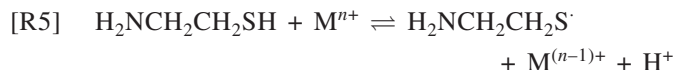
Fig. 4. $[I^-]$ effect on the iodate oxidation of CA. The effect of iodide can be seen on the reduced induction period and increased final absorbance of iodine as the iodide concentration is increased. $[CA]_0 = 0.005 \text{ mol L}^{-1}$, $[H^+]_0 = 0.02 \text{ mol L}^{-1}$, $[IO_3^-]_0 = 0.005 \text{ mol L}^{-1}$, $[I^-]_0 =$ (a) no iodide, (b) 0.00025, (c) 0.0005, (d) 0.00075, (e) 0.001 mol L^{-1} .



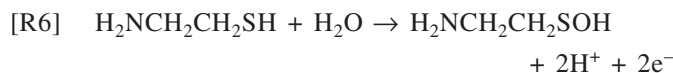
the optical observation of the iodine–CA reaction. Hence, data interpretation of the iodide effect was not possible, although a cursory glance showed that the iodide effect was mildly inhibitory.

Mechanism

The mechanistic basis of the oxidation of CA by iodate–iodine had fewer possible intermediates in going from CA (reactant) to cystamine (product) when compared with other organosulfur oxidations in which the oxidation pathway involves formation of sulfinic and sulfonic acids, as well as cleavage of the C–S bond to yield sulfate (28, 29). There are only two possible pathways towards formation of the dimer: through the cysteamine-thiyl radical (30) and (or) the cysteamine sulfenic acid. In metal-ion mediated oxidation of cysteamine, the radical pathway is highly favored (31).



Our reaction environment has been stripped of metal ions, making the radical pathway unlikely. Oxyiodine species are known to predominantly oxidize via two-electron steps, making the pathway through the unstable sulfenic acid the most likely pathway (32).



The sulfenic acid should rapidly combine with an unoxidized CA molecule (a condensation reaction) to form cystamine.

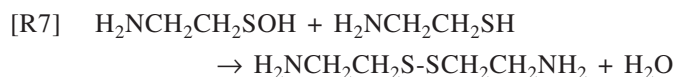
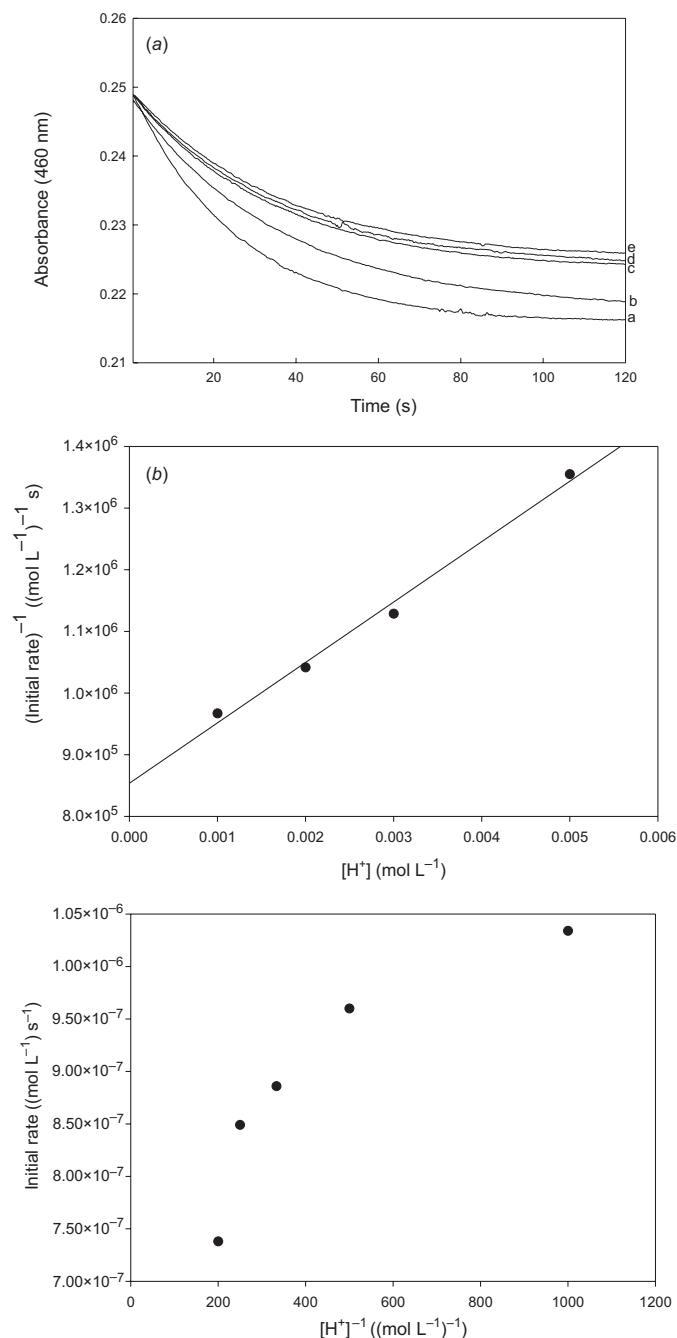
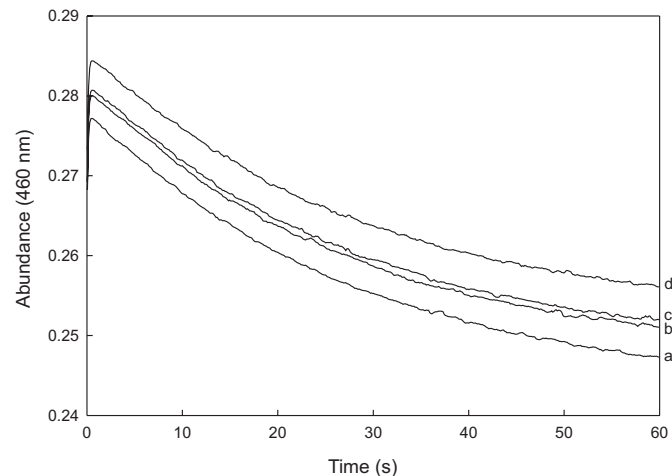


Fig. 5. (a) Effect of varying acid concentration on the reaction of CA and iodine. The initial rate of reaction decreases as the acid concentration is increased. $[CA]_0 = 0.001 \text{ mol L}^{-1}$, $[I_2]_0 = 0.00044 \text{ mol L}^{-1}$, $[H^+]_0 =$ (a) 0, (b) 0.001, (c) 0.002, (d) 0.003, (e) 0.004 mol L^{-1} ; (b) Plot of inverse of the initial rate vs. acid concentrations of the I_2 -CA reaction for low acid variations for the type of data shown in Fig. 5a. $[CA]_0 = 0.001 \text{ mol L}^{-1}$, $[I_2]_0 = 0.00044 \text{ mol L}^{-1}$; (c) Types of initial rates vs. inverse acid dependence plots for the I_2 -CA reaction for a wider range of acid concentrations than those selected for Fig. 5b. $[CA]_0 = 0.001 \text{ mol L}^{-1}$, $[I_2]_0 = 0.00044 \text{ mol L}^{-1}$.



Any uncondensed sulfenic acid left after all the CA has been consumed will rapidly disproportionate through standard pathways to form thiosulfonates (33) as well as CA.

Fig. 6. Effect of iodide variation on the I_2 -CA reaction. There is an increase in the initial absorbance with addition of iodide, but no parallel nature of the absorbance traces shows little effect of iodide on the reaction rate, only a change in the equilibrium position of the I_2 -CA reaction mixture. $[CA]_0 = 0.0002 \text{ mol L}^{-1}$, $[I_2]_0 = 0.00044 \text{ mol L}^{-1}$, $[I^-]_0 =$ (a) 4.0×10^{-5} , (b) 6.0×10^{-5} , (c) 8.0×10^{-5} , (d) $1.0 \times 10^{-4} \text{ mol L}^{-1}$.



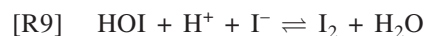
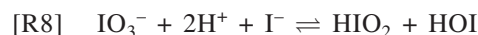
This can bring about some stoichiometric uncertainties, but if rxn., [R7] is very rapid, there will be very little deviation in the expected 1:6 stoichiometry.

Iodate oxidations are strongly acid-catalyzed and will not proceed except in low pH environments (34). All iodate oxidations reported in this manuscript were at pH conditions lower than 3.0. We expect, at these pH conditions, that the amino group of the cysteamine will be protonated and that the prevailing form of cysteamine will be $[H_3NCH_2CH_2SH]^+$. The accepted pK_a value of $[H_3NCH_2CH_2SH]^+$ is 10.8, with a K_b of the amino group of cysteamine as $6.3 \times 10^{10} \text{ (mol L}^{-1})^{-1}$, which calculates to a full protonation of the amino group in pH conditions lower than 4.0. Thus any further protonation to cysteamine will be in addition to the one already resident on the amino group. Since this protonation is distal to the active thiol group, it does not strongly influence its reactivity. We shall represent cysteamine, in this manuscript, however, as the neutral form.

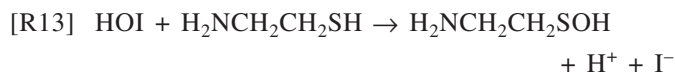
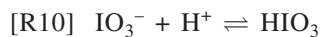
Sulfenic acids are stronger acids than thiols and, if they are long-lived, would exist predominantly as zwitterions (produced in rxn. [R6] and others), $^+N(H)_3CH_2CH_2SO^-$. However, the strongly acidic environment would protonate the oxygen atom, and it would exist predominantly as $^+N(H)_3CH_2CH_2SOH$.

Oxyiodine oxidizing species

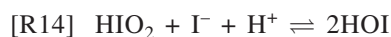
The chemistry of oxyiodine species has been extensively studied, and it is well-established that the major oxidizing species are HIO_2 , HOI , and molecular iodine (I_2). These species are derived from iodate through a series of well-known reactions (35, 36).



In the absence of iodide, the initiation reaction involves the direct oxidation of CA by iodic acid.

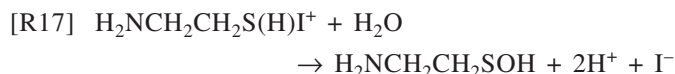


Equations [R10]–[R13] are relevant at the beginning of the reaction before iodide ions accumulate. After iodide concentrations have built up to effective levels, the reaction will proceed through rxn. [R8], as it is the overall rate-determining step in the consumption of CA. In the presence of added iodide ions, as in Fig. 4, eqs. [R10]–[R13] are completely shunted out and are insignificant. The sum of rxns. [R8] + [R10] + [R11] + [R12] + 2[R13] shows that in each initial reaction cycle, 1 mol of iodide ultimately produces 2 mol of iodide in a quadratic autocatalytic sequence. This is obvious because each iodate ion, whose reactivity is triggered off by iodide, will ultimately end up as iodide, effectively doubling the number of iodide ions initially present. Reaction [R13] is the major oxidation route. This leaves two important oxyiodine reactions, which involve the disproportionation of HOI (37). This disproportionation ensures that there is no accumulation of HOI in the reaction medium, especially after all the reducing substrate has been consumed. The stable species allowable at the end of the reaction are iodate, iodine, and iodide.

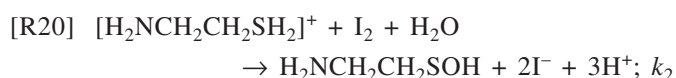
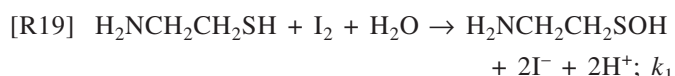
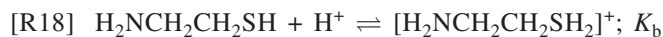


Iodine oxidation

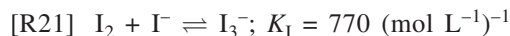
Acid dependence experiments (Figs. 5a and 5b) clearly indicate an electrophilic mechanism with an initial attack by iodine on the nucleophilic sulfur atom of CA.



The product is then formed by rxn. [R7]. This step ([R16] + [R17]) was qualitatively proved by the experimental observations of an immediate drop in pH upon mixing iodine and CA. Thus, acid dependence experiments can be justified from the basis of an initial protonation of the thiol group, which subsequently reacts much more slowly with the electrophilic iodine atom.



In this reaction scheme we are ignoring the iodine–triiodide equilibrium (38, 39) by assuming that triiodide reacts just as rapidly as iodine.



This assertion was based on our experiments that showed that the effect of iodide on the reaction rate was inconclusive. Addition of iodide to the reaction medium changed the original absorbance, but did not alter the subsequent rate of consumption of iodine (see Fig. 6).

Using [R18]–[R20], we can derive the following overall rate law for the consumption of iodine.

$$[\text{1}] \quad \text{Rate} = -\frac{d[\text{I}_2]}{dt} = \frac{[\text{CA}]_0[\text{I}_2]}{(1 + K_b[\text{H}^+])} (k_1 + k_2 K_b[\text{H}^+])$$

In eq. [1], $[\text{CA}]_0$ represents the amount of cysteamine added to the reaction mixture. This is then partitioned between the protonated and unprotonated forms of the thiol, based on the acid concentrations and K_b . Equation [1] will give different acid dependence behavior depending upon the relative values of k_1 and k_2 . If $k_1 \gg k_2$, the general form of the equation for the initial rate of reaction vs. the inverse of the acid concentration will give a nearly straight line at acid concentrations where $K_b[\text{H}^+] \ll 1$, with the second term in eq. [1] assumed to be negligible. The plot shown in Fig. 5b was restricted to low acid concentrations. The high acid concentration kinetics data were discarded. The low acid concentrations plot allows us to estimate the values of k_1 and K_b by assuming that the observed retardation is due to the removal of active cysteamine by the protonation equilibrium. After deleting the second term in eq. [1], the equation can then be rearranged and written as:

$$[\text{2}] \quad \frac{1}{\text{mod}(\text{rate})} = \left(\frac{K_b}{k_1[\text{CA}]_0[\text{I}_2]_0} \right) [\text{H}^+] + \left(\frac{1}{k_1[\text{CA}]_0[\text{I}_2]_0} \right)$$

Equation [2] is then used to plot the inverse of the modulus of the initial rate vs. the acid concentrations (see Fig. 5b), from where we can evaluate values of k_1 and K_b . From the intercept, a value of $k_1 = 2.7 \pm 0.3 \text{ (mol L}^{-1}\text{)}^{-1} \text{ s}^{-1}$ was deduced. The slope gave $K_b = 117 \pm 15 \text{ (mol L}^{-1}\text{)}^{-1}$. This value of K_b has no thermodynamic significance apart from the fact that it fits kinetics data through eq. [2]. This is a value that is only relevant for the conditions used for Figs. 5a and 5b. Literature quotes the $\text{p}K_a$ of the thiol group of cysteamine as 8.6, but the protonation of the amino group precludes an accurate measurement of $\text{p}K_a$ for $[\text{H}_2\text{NCH}_2\text{CH}_2\text{SH}_2]^+$, should this exist. Another possible mechanism for the observed acid retardation of iodine oxidation is the loss of nucleophilicity of the water molecules, owing to the formation of the hydronium ions. However, this retardation would be kinetically indistinguishable to the one suggested through rxn. [R20]. A plot of inverse acid dependence, which includes both high and low acid concentrations, is shown in Fig. 5c. This is not a linear plot, as expected from the form of eq. [1]. We could then work with the curve generated in Fig. 5c and curve-fit it to variables k_1 , k_2 , and K_b . This fitting procedure gave $k_2 = 0.37 \text{ (mol L}^{-1}\text{)}^{-1} \text{ s}^{-1}$.

Table 1. Cysteamine–iodate–iodine reaction.

Reaction No.	Reaction	k_f and k_t
M1	$\text{H}^+ + \text{IO}_3^- \rightleftharpoons \text{HIO}_3$	$1 \times 10^7, 1 \times 10^9$
M2	$\text{HIO}_3 + \text{RSH} \rightarrow \text{HIO}_2 + \text{RSOH}$	2.5×10^2
M3	$\text{HIO}_2 + \text{RSH} \rightarrow \text{HOI} + \text{RSOH}$	5×10^2
M4	$\text{HOI} + \text{RSH} \rightarrow \text{I}^- + \text{H}^+ + \text{RSOH}$	1×10^3
M5	$\text{RSOH} + \text{RSH} \rightarrow \text{RSSR} + \text{H}_2\text{O}$	5×10^8
M6	$\text{IO}_3^- + \text{I}^- + 2\text{H}^+ \rightleftharpoons \text{HIO}_2 + \text{HOI}$	$2.8, 1.44 \times 10^3$
M7	$\text{HIO}_2 + \text{I}^- + \text{H}^+ \rightleftharpoons 2\text{HOI}$	$2.1 \times 10^8, 90$
M8	$\text{HOI} + \text{I}^- + \text{H}^+ \rightleftharpoons \text{I}_2 + \text{H}_2\text{O}$	$3.1 \times 10^{12}, 2.2$
M9	$\text{IO}_3^- + \text{HOI} + \text{H}^+ \rightleftharpoons 2\text{HIO}_2$	$8.6 \times 10^2, 2.00$
M10	$\text{I}_2 + \text{I}^- \rightleftharpoons \text{I}_3^-$	$6.2 \times 10^9, 8.5 \times 10^6$
M11	$\text{I}_2 + \text{RSH} + \text{H}_2\text{O} \rightarrow \text{RSOH} + 2\text{H}^+ + 2\text{I}^-$	2.7
M12	$\text{I}_3^- + \text{RSH} + \text{H}_2\text{O} \rightarrow \text{RSOH} + 2\text{H}^+ + 3\text{I}^-$	1.5
M13	$\text{RSH} + \text{H}^+ \rightleftharpoons \text{RSH}_2^+$	$1 \times 10^8, 8.5 \times 10^5$
M14	$\text{RSH}_2^+ + \text{I}_2 + \text{H}_2\text{O} \rightarrow \text{RSOH} + 3\text{H}^+ + 2\text{I}^-$	0.37

Note: RSH = cysteamine; RSOH = unstable cysteamine sulfenic acid intermediate; RSSR = cystamine.

Computer modeling

The reaction scheme was modeled using the Kintecus software generated by James Ianni. The whole reaction scheme is shown in Table 1. The 14-reaction scheme was able to model satisfactorily all of the reaction dynamics observed in Figs. 1–4. The data for the direct reaction of iodine and CA could also be simulated by the same model after nullifying rxns. [M1]–[M7] (i.e., setting all their rate constants to zero).

Charge-transfer complexes

While the calculations were able to simulate the general dynamics of the data shown in Figs. 1–4, they gave much lower absorbance readings than those shown in these figures. The absorbance readings only matched the calculations at the beginning and at the end of the simulations. The experimentally observed intermediate values were much higher, owing to the expected charge-transfer complexes that cysteamine is known to form with molecular iodine (23, 40).

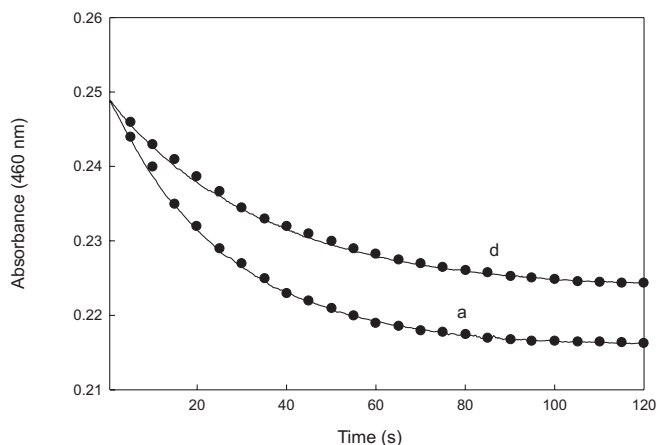


Absorbance readings from experiments and simulations coincided under conditions where iodate was in stoichiometric excess over cysteamine such that at the end of the reaction cysteamine concentrations had vanished, thus precluding the possibility of rxn. [R22]. While reactions of the [R22]-type have been reported (40), no specific measurements have been performed for the cysteamine–iodine mixtures. Reaction [R22] is suppressed in high acid conditions, such that it was easier to fit simulations to the data in Fig. 5a. Figure 7 shows a typical fit to the experimental data in Fig. 5a at separate acid concentrations.

Adoption of rate constants

The model presented had very few rate constants that needed to be guessed for the best simulations fit. For example, kinetics constants for reactions [M6]–[M10] were obtained from well-established literature values (27, 35, 37, 41, 42). In the absence of added iodide ions (as in data in Fig. 4), the most important reaction in the whole model was

Fig. 7. Comparison of experimental and calculated absorbance traces for the I_2 –CA reaction data shown in Fig. 5a (traces a and d). The symbols represent calculations.



[M2]. After setting up an initial guess value for $k_{\text{M}2}$, the kinetics parameters for the rest of the reactions in that chain, [M3] and [M4], became instantly irrelevant for as long as they were faster than the set value for $k_{\text{M}2}$ and with the relative magnitudes in the order of $k_{\text{M}3} < k_{\text{M}4}$. Any reversal in this order generated large amounts of HIO_2 (in excess iodate conditions), which never decayed as the reaction reached its end point with respect to iodine production. The data shown in Fig. 4 could be modeled without reactions [M1] through [M4]. We settled on a value of $k_{\text{M}2}$ of $250 \text{ (mol L}^{-1}\text{)}^{-1} \text{ s}^{-1}$ as the one that gave us the best fit to the induction period. The two protolytic reactions, [M1] and [M13], were set to be faster than all reactions in the mechanism. The role of [M1] was to ensure bimolecular kinetics for rxn. [M2]. The role of [M13] was to simulate acid retardation observed in the direct oxidation of CA by iodine. The values of $k_{\text{M}13}$ and $k_{-\text{M}13}$ were linked together by the value of K_b derived in this study. The fact that reaction [M13] was rapid in both directions made it insignificant with respect to the sequence [M1]–[M4], since $k_{\text{M}2}$, the rate-determining step for that sequence, was only $250 \text{ (mol L}^{-1}\text{)}^{-1} \text{ s}^{-1}$. The effect of sequence [M10] + [M12] was not utilized in the derivation of rate for

eq. [1] and was not very effective in the mechanism for the overall iodate–CA reaction. A very small degree of retardation was observed in the iodine–CA reaction upon asserting this sequence (see Fig. 6). The possible direct reaction of the protonated thiol with triiodide was also not included in the mechanism.

Conclusion

Our study shows that cysteamine, the well-known precursor to taurine (14), is not easily oxidized to taurine by the mild oxidizing agent iodine and without the standard P450-type enzymes and the flavin-containing monooxygenases (43). In its goitrogenic role (9), cysteamine most likely abstracts the iodine atom in a reversible process to form the disulfide, which can be converted back to the thiol by a very mild redox potential.

Acknowledgement

We would like to thank Itai Chipinda for performing the HPLC analysis for us. This work was supported by research grant Nos. CHE 0137435 and CHE 0341769 from the National Science Foundation and research grant No. R01 AI051509-01A2 from the National Institutes of Health.

References

1. R.B. Freedman. *FEBS Lett.* **97**, 201 (1979).
2. C.R. Chinake and R.H. Simoyi. *J. Phys. Chem.* **98**, 4012 (1994).
3. B. Kalyanaraman. *Biochem. Soc. Symp.* **61**, 55 (1995).
4. I.R. Wilson and G.M. Harris. *J. Am. Chem. Soc.* **82**, 4515 (1960).
5. I.R. Wilson and G.M. Harris. *J. Am. Chem. Soc.* **83**, 286 (1961).
6. J.M. Geelen, L.A. Monnens, and E.N. Levchenko. *Nephrol. Dial. Transplant.* **17**, 1766 (2002).
7. W.A. Gahl. *Eur. J. Pediatr.* **162** (Suppl. 1), S38 (2003).
8. R.L. Pisoni, G.Y. Park, V.Q. Velilla, and J.G. Thoene. *J. Biol. Chem.* **270**, 1179 (1995).
9. V.E. Kimonis, J. Troendle, S.R. Rose, M.L. Yang, T.C. Markello, and W.A. Gahl. *J. Clin. Endocrinol. Metab.* **80**, 3257 (1995).
10. F. Iwata, E.M. Kuehl, G.F. Reed, L.M. McCain, W.A. Gahl, and M.I. Kaiser-Kupfer. *Mol. Genet. Metab.* **64**, 237 (1998).
11. O.I. Aruoma, B. Halliwell, B.M. Hoey, and J. Butler. *Biochem. J.* **256**, 251 (1988).
12. D. Becker, S. Summerfield, S. Gillich, and M.D. Sevilla. *Int. J. Radiat. Biol.* **65**, 537 (1994).
13. M.M. Oosthuizen and D. Greyling. *Redox Rep.* **4**, 277 (1999).
14. D. Cavallini, C. De Marco, R. Scandurra, S. Dupre, and M. Graziani. *J. Biol. Chem.* **241**, 3189 (1966).
15. J.H. Fellman, T.R. Green, and A.L. Eicher. *Adv. Exp. Med. Biol.* **217**, 39 (1987).
16. G. Ricci, R. Chiaraluce, G. Pitari, S. Dupre, O. Fujii, Y. Hosokawa, and K. Yamaguchi. *J. Nutr. Sci. Vitaminol.* **35**, 143 (1989).
17. C.R. Chinake and R.H. Simoyi. *J. Phys. Chem. B*, **101**, 1207 (1997).
18. B.S. Martincigh, C. Mundoma, and R.H. Simoji. *J. Phys. Chem. A*, **102**, 9838 (1998).
19. R.H. Simoyi, K. Streete, C. Mundoma, and R. Olojo. *S. Afr. J. Chem.* **55**, 136 (2002).
20. C.C. Capen. *Toxicol. Lett.* **64/65**, 381 (1992).
21. C.J. Doona and D.M. Stanbury. *J. Phys. Chem.* **98**, 12630 (1994).
22. P.J. Hogg. *Redox Rep.* **7**, 71 (2002).
23. J.P. Danehy. *Q. Rep. Sulfur Chem.* **2**, 325 (1967).
24. J. Kurzawa and K. Janowicz. *Acta Chim. Hung.* **125**, 147 (1988).
25. G. Rabai and M.T. Beck. *J. Chem. Soc. Dalton Trans.* 1669 (1985).
26. M. Melicherik, A. Olexova, and L. Treindl. *J. Mol. Catal. A: Chem.* **127**, 43 (1997).
27. H.A. Liebhafsky and G.M. Roe. *Int. J. Chem. Kinet.* **11**, 693 (1971).
28. T.R. Chigwada, E. Chikwana, and R.H. Simoyi. *J. Phys. Chem. A*, **109**, 1081 (2005).
29. T.R. Chigwada and R.H. Simoyi. *J. Phys. Chem. A*, **109**, 1094 (2005).
30. T. Nauser and C. Schoneich. *Chem. Res. Toxicol.* **16**, 1056 (2003).
31. L. Pecci, G. Montefoschi, G. Musci, and D. Cavallini. *Amino Acids*, **13**, 355 (1997).
32. R. Okazaki and K. Goto. *Heteroat. Chem.* **13**, 414 (2002).
33. G. Capozzi and G. Modena. *Oxidation of thiols. In The chemistry of the thiol group. Edited by S. Patai. Wiley and Sons, New York. 1974. p. 791.*
34. Y. Xie, M.R. McDonald, and D.W. Margerum. *Inorg. Chem.* **38**, 3938 (1999).
35. G. Schmitz. *Phys. Chem. Chem. Phys.* **1**, 1909 (1999).
36. K. Kustin and M. Eigen. *J. Am. Chem. Soc.* **84**, 1355 (1962).
37. L. Kolaranic and G. Schmitz. *J. Chem. Soc. Faraday Trans.* **88**, 2343 (1992).
38. M.-F. Ruisse, J. Aubard, B. Galland, and A. Adenir. *J. Phys. Chem.* **90**, 4382 (1986).
39. D.H. Turner, G.W. Flynn, N. Sutin, and J.V. Beitz. *J. Am. Chem. Soc.* **94**, 1554 (1972).
40. W.H. Miller, R.O. Roblin, and E.B. Astwood. *J. Am. Chem. Soc.* **67**, 2201 (1945).
41. G. Schmitz. *Phys. Chem. Chem. Phys.* **2**, 4041 (2000).
42. E.T. Urbansky, B.T. Cooper, and D.W. Margerum. *Inorg. Chem.* **36**, 1338 (1997).
43. W.X. Guo, L.L. Poulsen, and D.M. Ziegler. *Biochem. Pharmacol.* **44**, 2029 (1992).